FULL PAPER

Dalton
www.rsc.org/dalton

Nitrido-ruthenium(VI) and -osmium(VI) complexes of multianionic chelating (N, O) ligands. Reactions with nucleophiles, electrophiles and oxidizing agents †

Ka-Lai Yip, Wing-Yiu Yu, Pui-Ming Chan, Nian-Yong Zhu and Chi-Ming Che *
Department of Chemistry and Open Laboratory of Chemical Biology of the Institute of Molecular Technology for Drug Discovery and Synthesis, The University of Hong Kong, Pokfulam Road, Hong Kong

Received 1st May 2003, Accepted 10th July 2003
First published as an Advance Article on the web 5th August 2003

This account presents the diverse reactivity of nitridoruthenium(VI) complexes with nucleophilic, electrophilic and oxidizing agents. $[Ru^{VI}(N)(L^1)Cl]$ (**1**) [H_2L^1 = 2,6-bis(2,2-diphenyl-2-hydroxyethyl)pyridine] reacted with excess phosphines such as PPh_3, $PPhMe_2$ and dppe to give $[Ru^{III}(HL^1)(PPh_3)Cl_2]$ (**2a**), $[Ru^{III}(L^1)(PPhMe_2)_2Cl]$ (**2b**) and $[Ru^{III}(L^1)(dppe)Cl]$ (**2c**), respectively. In the presence of py or Hpz, **1** was converted to $[Ru^{III}(L^1)(py)_2Cl]$ (**3a**) and $[Ru^{III}(L^1)(Hpz)_3]Cl$ (**3b**), respectively. A dinuclear μ-nitridoruthenium complex, $[Ru^{IV}(L^1)Cl_2(\mu\text{-}N)Ru^{VI}(L^1)\text{-}(C_8H_{10}N)Cl]$ (**4**), was obtained by treating **1** with 2,6-dimethylaniline. Based on X-ray crystallographic study, the compound is characterized by an unsymmetrical Ru–N≡Ru moiety with the measured Ru–N distances being 1.661(5) and 1.837(5) Å. Complex **1** reacted with dmf to give $[Ru^{III}(HL^1)(dmf)Cl_2]$ (**5**) in 17% yield. Excess $(Me_3O)BF_4$ reacted with **1** to give a dinuclear μ-OH ruthenium complex, $[Ru_2(N)_2(L^1)_2(OH)]PF_6$ (**6**). The measured $Ru\text{–}O_{(OH)}$ distance is 1.984(3) Å and the average Ru–O–Ru angle was found to be 100.4(2)°. Other nitrido-metal complexes, $[n\text{-}Bu_4N]\text{-}[M^{VI}(N)(L)]$ [L = L^2 and L^3; M = Os and Ru; H_4L^2 = 1,2-dichloro-4,5-bis(2-hydroxybenzamido)benzene, H_4L^3 = 1,2-bis(2-hydroxybenzamido)benzene], underwent ligand protonation to form $[M^{VI}(N)(HL)]$ complexes, which have been characterized by X-ray crystallography. Oxidation of $[n\text{-}Bu_4N][Os^{VI}(N)(L^2)]$ by $PhI(OAc)_2$ produced $[n\text{-}Bu_4N][Os^{VI}(N)(L^2O_2)]$ (**8**) in 10% yield. X-ray structure analysis of **8** showed that the coordinated phenoxy moiety was converted to a benzoquinone moiety while the Os≡N group remained intact.

Introduction

There is a growing interest in the chemistry of metal-nitrido complexes, particularly those of late transition metals.[1] Recently Meyer,[2] Mayer[3] and Lau[4] have independently explored some interesting reactivities of $[Os^{VI}(N)(terpy)Cl_2]^+$ (terpy = 2,2′:6′,2″-terpyridine), $[Os^{VI}(N)(Tp)Cl_2]^+$ [Tp = hydrotris-(1-pyrazolyl)borate] and $[Os^{VI}(N)(salen)]^+$ complexes. Reminiscent of the oxo-metal complexes, these nitridoosmium(VI) complexes undergo proton-coupled electron transfer[5,6] and atom transfer reactions.[2,3,4b] Some other reactivity patterns such as nitrido coupling reactions and electrochemistry had previously been examined by us and others.[7–9] In view of the earlier works by Groves[10] and Carriera[11] that nitridomanganese(V) complexes can effect alkene aziridination and the rich oxidation chemistry of high-valent oxo-ruthenium complexes,[12] we investigate the reactivity of nitridoruthenium(VI) complexes for potential hydrocarbon functionalization.[13] To our knowledge, studies on nitridoruthenium(VI) complexes are sparse in the literature.[13,14] Previously, we reported preparation and structural characterization of a series of nitrido-ruthenium(VI) and -osmium(VI) complexes containing multianionic chelating (N, O) ligands (Fig. 1).[14b] The reactivities of the complexes toward triphenylphosphine were found to be affected by the electron-donating strength of the auxiliary ligands. Herein, we present a comprehensive account on the reactivity of nitrido-ruthenium(VI) complexes with respect to their reactions with nucleophilic and electrophilic reagents.

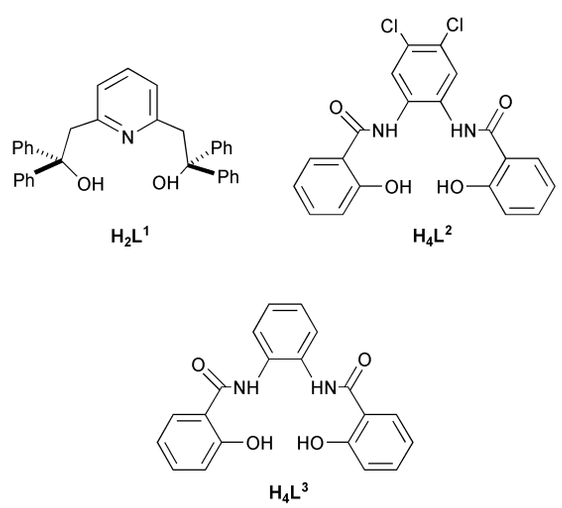

Fig. 1 Multi-anionic chelating (N, O) ligands.

Experimental

Materials

All solvents were purified by standard methods before use. The compounds $[Ru^{VI}(N)(L^1)Cl]$, $[n\text{-}Bu_4N][Ru^{VI}(N)(L^2)]$, $[n\text{-}Bu_4N]\text{-}[Os^{VI}(N)(L^2)]$, $[n\text{-}Bu_4N][Ru^{VI}(N)(L^3)]$ and $[n\text{-}Bu_4N][Os^{VI}(N)\text{-}(L^3)]$ were prepared according the previously reported methods.[14b] Triphenylphosphine, dimethylphenylphosphine, 1,2-bis(diphenylphosphino)ethane, morpholine, piperidine, pyridine, pyrazole, 2,6-dimethylaniline, trimethyloxonium tetrafluoroborate and iodosylbenzene diacetate were obtained commercially and used as received.

Instrumentation

Infrared spectra were recorded as a KBr disc or Nujol mull on a Nicolet 20 SXC FT-IR spectrophotometer. UV-VIS spectra were recorded on a HP 8452A diode array spectrophotometer. FAB-MS spectra were obtained from a Finnigan MAT 95 mass spectrometer using 3-nitrobenzyl alcohol as matrix. Electrospray ionization (ESI) mass spectrometry was performed on a Finnigan LCQ quadrupole ion trap mass spectrometer. NMR spectra were obtained using Bruker DPX-300 and -500 pulsed

† Electronic supplementary information (ESI) available: Fig. S1–S6. See http://www.rsc.org/suppdata/dt/b3/b304920p/

DOI: 10.1039/b304920p

Fourier transform instruments. Elemental analyses were performed by the Institute of Chemistry of the Chinese Academy of Sciences.

X-Ray crystallography

X-Ray diffraction data were collected on a Enraf-Nonius CAD-4, Rigaku AFC7R or MAR diffractometer using graphite-monochromatized Mo-Kα radiation (λ = 0.71073 Å) at 301 K. Intensity data were corrected for Lorentz-polarization effects, and the structures were solved by the Patterson method and expanded by the Fourier methods (PATTY).[15] Structure refinements were performed by the full-matrix least squares using the software package TEXSAN[16] on a Silicon Graphics Indy computer. The structures of **2a**–**c**, **3a**–**b**, **4**, **5**, **6**, **7** and **8** were established by X-ray crystallography; the crystal data, selected bond distances and angles are listed in Tables 1 and 2.

CCDC reference numbers 209727–209736, 213055 and 213056.

See http://www.rsc.org/suppdata/dt/b3/b304920p/ for crystallographic data in CIF or other electronic format.

Syntheses

[$Ru^{III}(HL^1)(PPh_3)Cl_2$] (2a). To a degassed MeOH solution (10 cm^3) containing **1** (100 mg, 0.16 mmol) was added PPh_3 (127 mg, 0.48 mmol) under an argon atmosphere with stirring, an instantaneous color change from purple to red occurred. The reaction mixture was stirred for 3 h and the resultant brown solution was rotary evaporated to dryness to give a brown solid. The brown residue was recrystallized by slow diffusion of Et_2O to a CH_2Cl_2 solution to afford a yellow crystalline solid. Yield = 28 mg, 19%. Found: C, 66.23; H, 4.76; N, 1.51. $C_{51}H_{42}NO_2PCl_2Ru{\cdot}H_2O$ requires C, 66.45; H, 4.81; N, 1.52%. IR (KBr, cm^{-1}): 3060, 2935, 1438, 1190, 1120 and 1022. FAB-MS (+ve): *m*/*z* 868 ($M^+ - Cl$).

[$Ru^{III}(L^1)(PPhMe_2)_2Cl$] (2b). To a CH_2Cl_2 solution (20 cm^3) of **1** (100 mg, 0.16 mmol) was added $PPhMe_2$ (55 mg, 0.48 mmol) under an argon atmosphere. The yellow-orange reaction mixture was stirred for 2 h at room temperature to give a pale yellow solution. After removal of solvent by rotary evaporation, the pale yellow residue was recrystallized by slow diffusion of Et_2O to a CH_2Cl_2 solution to give a yellow crystalline solid. Yield = 117 mg, 83%. Found: C, 66.9; H, 5.75; N, 1.55. $C_{49}H_{49}NO_2P_2ClRu$ requires C, 66.7; H, 5.6; N, 1.59%. IR (Nujol, cm^{-1}): 2850, 1600, and 1575. FAB-MS (+ve): *m*/*z* 882 ($M^+ - Cl$).

[$Ru^{III}(L^1)(dppe)Cl$] (2c). To a degassed MeOH solution (20 cm^3) of **1** (100 mg, 0.16 mmol) was added dppe (193 mg, 0.48 mmol) under an argon atmosphere. The purple reaction mixture was stirred for 3 h at room temperature to give a yellow-brown solution. Removal of solvent by rotary evaporation afforded a brown residue, which was recrystallized by slow diffusion of Et_2O to a CH_2Cl_2 solution to give an orange solid. Yield = 35 mg, 22%. Found: C, 68.0; H, 5.24; N, 1.23. $C_{59}H_{51}NO_2P_2ClRu{\cdot}2H_2O$ requires C, 68.1; H, 5.33; N, 1.35%. IR (KBr, cm^{-1}): 3065, 3025, 2932, 1481, 1433 and 1097. FAB-MS (+ve): *m*/*z* 968 ($M^+ - Cl$).

[$Ru^{III}(L^1)(py)_2Cl$] (3a). A mixture of CH_2Cl_2 (10 cm^3) and pyridine (1 cm^3) was degassed by purging with argon for 5 min, and the solution was added dropwise to **1** (100 mg, 0.16 mmol) in a 50 cm^3 Schlenk flask under an argon atmosphere. The purple reaction mixture was stirred for 3 h at room temperature and the resultant yellow-brown solution was rotary evaporated to dryness to give a yellow-brown residue. The residue was then recrystallized by slow diffusion of Et_2O to a CH_2Cl_2 solution. Yield = 43 mg, 40%. Found: C, 63.2; H, 5.23; N, 5.15. $C_{43}H_{37}N_3O_2ClRu{\cdot}3H_2O$ requires C, 63.1; H, 5.3; N, 5.13%. IR

Table 1 Crystallographic data for **2a**–**c**, **3a**–**b**, **4**–**8**[a]

	2a	2b	2c	3a	3b	4	5	6	7·CH_3OH	8
Formula	$C_{51.5}H_{43}Cl_3NO_2PRu$	$C_{49}H_{49}NO_2ClP_2Ru$	$C_{59}H_{53}ClNO_3P_2Ru$	$C_{47}H_{49}ClN_3O_4Ru$	$C_{43}H_{45}ClN_7O_4Ru$	$C_{79}H_{77}Cl_4N_4O_5Ru_2$	$C_{39}H_{41}Cl_2N_3O_4Ru$	$C_{66}H_{54}N_4O_5F_6PRu_2$	$C_{20}H_{10}N_2O_5Cl_2Ru{\cdot}CH_3OH$	$C_{36}H_{46}Cl_2N_4O_7Os$
M	946.26	882.4	1022.48	856.41	860.38	1506.39	787.72	1330.24	562.33	907.87
Crystal symmetry	Triclinic	Monoclinic	Monoclinic	Triclinic	Monoclinic	Triclinic	Triclinic	Monoclinic	Monoclinic	Monoclinic
Space group	$P\bar{1}$	$P2_1/n$ (no. 14)	$C2/c$	$P\bar{1}$	$P2_1/c$	$P\bar{1}$	$P\bar{1}$ (no.1)	$P2_1/n$ (no. 14)	$P2_1/n$ (no. 14)	$P2_1/n$
a/Å	15.254(2)	9.243(3)	49.377(10)	10.239(2)	9.621(2)	13.498(3)	10.098(2)	17.8677(3)	12.963(2)	13.732(3)
b/Å	17.659(2)	11.208(4)	9.465(19)	13.922(3)	35.268(7)	16.684(3)	14.093(3)	19.0282(2)	13.707(2)	18.256(4)
c/Å	19.344(3)	40.92(1)	21.639(4)	16.454(3)	11.953(2)	17.009(3)	14.192(3)	18.8130(3)	13.287(2)	15.546(3)
α/°	75.31(2)			100.42(3)		84.49(3)	66.68(2)			
β/°	70.65(2)	91(3)	104.48(3)	106.97(3)	97.79(3)	74.35(3)	79.25(2)	107.10(1)	117.85(2)	99.81(3)
γ/°	69.06(2)			107.30(3)		77.09(3)	87.84(2)			
V/Å^3	4537.3(11)	4238(2)	9792(3)	2047.8(7)	4018.4(13)	3592.7(12)	1820.7(7)	6113.5(2)	2087.4(7)	3840.3(14)
Z	4	4	8	2	4	2	2	4	4	4
Data collected	14465	6552	7761	5588	6103	8687	6364	41573	3958	4308
Data used	10368	2638	5230	3929	4089	5448	5419	12505	2825	2536
μ(Mo-Kα)/mm^{-1}	0.598	0.549	0.487	0.496	0.508	0.623	0.622	0.591	1.05	3.511
R_1	0.054	0.077	0.053	0.046	0.047	0.049	0.04	0.047	0.038	0.039
wR_2	0.15	0.10	0.14	0.12	0.13	0.13	0.12	0.08	0.049	0.097

[a] $R_1 = \Sigma||F_o| - |F_c||/\Sigma|F_o|$; $wR_2 = [\Sigma w(|F_o| - |F_c|)^2/\Sigma wF_o^2]^{1/2}$ where $w = 4F_o^2/\sigma^2(F_o^2)$.

Table 2 Selected bond distances (Å) and angles (°) for **2a**–**c**, **3a**–**b**, **4**–**8**

Complex **2a**			
Ru–N	2.17(4)	Ru–P	2.348(15)
Ru–O(1)	1.974(3)	Ru–Cl(1)	2.358(12)
Ru–O(2)	2.123(3)	Ru–Cl(2)	2.392(13)
N–Ru–O(1)	91.86(14)	O(1)–Ru–O(2)	176.9(1)
N–Ru–O(2)	88.49(13)	O(1)–Ru–P	87.6(1)
N–Ru–P	179.3(1)	O(2)–Ru–P	92.08(9)
Complex **2b**			
Ru–Cl(1)	2.431(4)	Ru–P(2)	2.415(4)
Ru–O(1)	2.001(9)	Ru–N(1)	2.13(1)
Ru–O(2)	2.008(9)	O(1)–C(17)	1.39(2)
Ru–P(1)	2.326(5)	O(2)–C37)	1.45(2)
Cl(1)–Ru–P(2)	174.3(1)	P(1)–Ru–O(1)	89.2(3)
P(1)–Ru–N(1)	171.5(3)	P(1)–Ru–O(2)	85.3(3)
O(1)–Ru–O(2)	173.3(4)	P(2)–Ru–O(1)	85.5(3)
Cl(1)–Ru–P(1)	84.9(2)	P(2)–Ru–N(1)	94.9(3)
Cl(1)–Ru–O(1)	89.0(3)	P(2)–Ru–O(2)	90.9(3)
Cl(1)–Ru–N(1)	86.8(3)	O(1)–Ru–N(1)	92.3(5)
Cl(1)–Ru–O(2)	94.4(3)	O(2)–Ru–N(1)	93.7(5)
P(1)–Ru–P(2)	93.5(2)		
Complex **2c**			
Ru–N	2.183(4)	Ru–P(1)	2.348(13)
Ru–O(1)	2.020(3)	Ru–P(2)	2.338(14)
Ru–O(2)	2.010(3)	Ru–Cl	2.447(14)
N–Ru–O(1)	88.38(14)	N–Ru–P(2)	173.2(1)
N–Ru–O(2)	90.97(13)	O(1)–Ru–O(2)	170.58(13)
N–Ru–P(1)	98.8(1)	P(1)–Ru–P(2)	81.89(5)
Complex **3a**			
Ru–N(1)	2.084(4)	Ru–O(1)	1.999(3)
Ru–N(2)	2.103(4)	Ru–O(2)	1.987(4)
Ru–N(3)	2.126(4)	Ru–Cl	2.395(14)
N(1)–Ru–N(2)	175.80(14)	N(1)–Ru–O(2)	92.28(15)
N(1)–Ru–N(3)	96.55(16)	N(3)–Ru–Cl	172.88(13)
N(1)–Ru–O(1)	93.07(15)	O(1)–Ru–O(2)	173.3(1)
Complex **3b**			
Ru–N(1)	2.073(4)	Ru–N(6)	2.089(3)
Ru–N(2)	2.101(3)	Ru–O(1)	1.974(3)
Ru–N(4)	2.086(4)	Ru–O(2)	2.003(3)
N(1)–Ru–N(4)	177.05(14)	N(1)–Ru–N(6)	90.73(14)
N(1)–Ru–O(1)	95.54(14)	N(2)–Ru–N(6)	179.51(16)
N(1)–Ru–O(2)	94.43(14)	O(1)–Ru–O(2)	169.94(12)
Complex **4**			
Ru(1)–N(1)	1.661(5)	Ru(2)–N(1)	1.837(5)
Ru(1)–N(2)	2.175(5)	Ru(2)–N(4)	2.153(5)
Ru(1)–N(3)	2.077(5)	Ru(2)–O(4)	1.943(4)
Ru(1)–O(2)	1.906(5)	Ru(2)–O(5)	2.003(4)
Ru(1)–O(3)	1.919(4)		
Ru(1)–N(1)–Ru(2)	170.7(3)	N(2)–Ru(1)–N(3)	177.15(17)
N(1)–Ru(2)–N(4)	175.4(2)	O(4)–Ru(2)–O(5)	178.59(16)
N(1)–Ru(1)–O(2)	114.9(2)	Cl(11)–Ru(2)–Cl(12)	174.36(7)
N(1)–Ru(1)–O(3)	118.6(2)		
Complex **5**			
Ru–N(1)	2.073(3)	Ru–Cl(1)	2.384(10)
Ru–O(1)	2.127(2)	Ru–Cl(2)	2.38(1)
Ru–O(2)	1.927(2)	C(34)–O(3)	1.234(4)
Ru–O(3)	2.119(2)	C(34)–N(2)	1.298(5)
N(1)–Ru–O(3)	177.4(1)	O(2)–Ru–O(3)	177.4(1)
N(1)–Ru–O(1)	92.3(1)	Cl(1)–Ru–Cl(2)	172.66(3)
N(1)–Ru–O(2)	95.33(10)	O(3)–Ru–C(34)	120.7(2)
O(2)–Ru–O(1)	172.35(9)		
Complex **6**			
Ru(1)–N(1)	1.603(4)	Ru(2)–N(2)	1.613(4)
Ru(1)–O(1)	2.032(3)	Ru(2)–O(1)	2.040(3)
Ru(1)–O(2)	1.934(3)	Ru(2)–O(4)	1.93(3)
Ru(1)–O(3)	1.928(3)	Ru(2)–O(5)	1.923(3)
Ru(1)–N(3)	2.096(4)	Ru(2)–N(4)	2.086(3)
Ru(1)–O(1)–Ru(2)	136(1)	N(4)–Ru(2)–O(4)	89.8(1)
N(1)–Ru(1)–O(1)	100.1(2)	N(4)–Ru(2)–O(5)	92.9(1)
N(2)–Ru(2)–O(1)	100.6(2)	N(3)–Ru(1)–O(1)	164.94(12)
N(3)–Ru(1)–O(2)	92.4(1)	O(1)–Ru(2)–N(4)	163.79(12)
N(3)–Ru(1)–O(3)	93.66(13)		
Complex **7**			
Ru–N(1)	1.599(4)	O(3)–C(7)	1.296(5)
Ru–O(1)	1.964(3)	O(4)–C(14)	1.210(6)
Ru–O(2)	1.975(3)	N(2)–C(7)	1.326(5)
Ru–N(2)	2.029(4)	N(3)–C(14)	1.395(6)
Ru–N(3)	1.988(3)		
N(1)–Ru–O(1)	110.4(2)	O(1)–Ru–N(2)	90.8(1)
N(1)–Ru–O(2)	106.4(2)	O(1)–Ru–N(3)	142.7(1)
N(1)–Ru–N(2)	102.7(2)	O(2)–Ru–N(2)	150.8(1)
N(1)–Ru–N(3)	106.9(2)	O(2)–Ru–N(3)	91.6(1)
O(1)–Ru–O(2)	78.3(1)	N(2)–Ru–N(3)	80.8(1)
Complex **8**			
Os–N(1)	1.625(9)	C(14)–C(15)	1.350(16)
Os–N(2)	1.974(9)	C(15)–C(16)	1.446(16)
Os–N(3)	1.854(13)	C(16)–C(17)	1.463(17)
Os–O(1)	2.007(7)	C(17)–C(18)	1.350(17)
Os–O(2)	2.014(8)	C(18)–C(19)	1.438(18)
O(5)–C(16)	1.223(13)	C(14)–C(19)	1.522(16)
O(6)–C(19)	1.252(14)		
N(1)–Os–O(1)	103.7(4)	N(2)–Os–O(2)	155.9(3)
N(1)–Os–O(2)	101.7(4)	N(3)–Os–O(1)	155.1(3)
N(2)–Os–O(1)	93.2(4)	N(3)–Os–O(2)	94.7(4)

(KBr, cm^{-1}): 3206, 3054, 2956, 1601, 1445 and 1045. ESI-MS (+ve): *m*/*z* 650 ($M^+ - Cl - py$).

$[Ru^{III}(L^1)(Hpz)_3]Cl$ (3b). A 25 cm^3 round-bottom flask was charged with **1** (100 mg, 0.16 mmol), pyrazole (109 mg, 1.6 mmol) and CH_2Cl_2 (20 cm^3) to give an orange-brown suspension. The suspension was stirred for 2 h at room temperature to afford a homogeneous dark brown solution. Complete removal of solvent by rotary evaporation gave a brown solid, which was recrystallized by slow diffusion of Et_2O to a MeOH solution to afford a dark brown crystalline solid. Yield = 40 mg, 31%. Found: C, 60.2; H, 5.32; N, 11.29. $C_{42}H_{39}N_7O_2ClRu{\cdot}H_2O{\cdot}CH_3OH$ requires C, 60.03; H, 5.27; N, 11.4%. IR (KBr, cm^{-1}): 3324, 3131, 2936, 2850, 1460, 1439 and 1046. FAB-MS (+ve): *m*/*z* 639 ($M^+ - Cl - 2Hpz$).

$[Ru^{IV}(L^1)Cl_2(\mu\text{-}N)Ru^{VI}(L^1)(DMA)]$ (4) [DMA = 2,6-dimethylaniline]. To a CH_2Cl_2 solution (20 cm^3) of **1** (100 mg 0.16 mmol) was added DMA (0.059 cm^3, 0.48 mmol) at ambient temperature, an instantaneous color change from purple to red-brown occurred. After stirring for 3 h, the reaction mixture was rotary evaporated to dryness to give a red-brown solid. The solid was recrystallized by diffusion of Et_2O into a CH_2Cl_2 solution to give a red-brown crystal. Yield = 20 mg, 9%. UV-VIS (CH_2Cl_2), λ_{max}/nm (ε/dm^3 mol^{-1} cm^{-1}): 258 (sh) (56234), 354 (sh) (20417), 523 (11481). Found: C, 64.9; H, 5.06; N, 3.98. $C_{74}H_{65}N_4O_4Ru_2Cl_2{\cdot}H_2O$ requires C, 65.1; H, 4.95; N, 4.1%. IR (KBr, cm^{-1}): 3056, 2917, 1606, 1039 and 1008. NMR, δ_H (500 MHz; 277 K; solvent $CDCl_3$; standard TMS): 1.86–2.46 (8H, m, $4CH_2$), 3.75 (6H, s, $2CH_3$), 6.52–7.84 (49H, m). ESI-MS (+ve): *m*/*z* 1347 ($M^+ - H$).

$[Ru^{III}(HL^1)(dmf)Cl_2]$ (5). A dmf solution (10 cm^3) of **1** (1 g, 1.6 mmol) was stirred at room temperature for 24 h. The red-brown solution was concentrated by rotary evaporation to *ca.* 5 cm^3 and the titled complex was isolated as a crystalline solid by slow diffusion of Et_2O into a dmf solution. Yield = 0.24 g, 17%. Found: C, 55.8; H, 5.78; N, 5.18. $C_{39}H_{41}N_3O_4$-

$Cl_2Ru{\cdot}3H_2O$ requires C, 55.7; H, 5.63; N, 4.99%. IR (KBr, cm^{-1}): 3055, 2917, 1655 (CO) and 1639 (CO). FAB-MS (+ve): *m*/*z* 606 (M^+ − dmf − Cl).

$[Ru^{VI}_2(N)_2(L^1)_2(OH)]PF_6$ (6). To a CH_2Cl_2 solution (10 cm^3) of **1** (100 mg, 0.16 mmol) was added excess $(Me_3O)BF_4$ (300 mg) under an argon atmosphere. After stirring the mixture for 5 h, the resulting red solution was filtered and the filtrate was evaporated to dryness by vacuum. The residual solid was dissolved in MeOH and ammonium hexafluorophosphate (300 mg) was added. After standing the solution for overnight at room temperature, a red crystalline solid was formed and was collected on a frit. Yield = 72 mg, 67%. Found: C, 59.7; H, 4.33; N, 4.38. $C_{66}H_{55}N_4O_5PF_6Ru_2$ requires C, 59.6; H, 4.16; N, 4.21%. IR (KBr, cm^{-1}): 3498 (OH), 2850, 1610, 1446 1042, and 854. NMR, δ_H (300 MHz, 298 K, $CDCl_3$, standard TMS): 4.05 [4H, d, (J = 15.2 Hz), $2CH_2$], 4.7 [4H, d, (J = 15.2 Hz), $2CH_2$], 7.10 (16H, m), 7.38 (24H, m), 7.61 (4H, m), 7.79 (1H, m), 8.13 (1H, m) and 9.93 (1H, s, 1 OH). FAB-MS (+ve): *m*/*z* 1185 (M^+).

$[Ru^{VI}(N)(HL^2)]$ (7) [H_4L^2: 1,2-dichloro-4,5-bis(2-hydroxybenzamido)benzene]. To a CH_2Cl_2 solution (10 cm^3) of [n-Bu_4N]-$[Ru^{VI}(N)(L^2)]$ (100 mg, 0.14 mmol) was added excess (Me_3O)-BF_4 (300 mg) under an argon atmosphere, and the mixture was stirred for 1 h at room temperature to give an orange precipitate. The solid was filtered and washed with CH_2Cl_2. Yield = 62 mg, 83%. Found: C, 45.3; H, 2.02; N, 7.78. $C_{20}H_{11}N_3O_4Cl_2Ru$ requires C, 45.4; H, 2.09; N, 7.94%. IR (KBr, cm^{-1}): 2930, 1600 (CO) and 1460. NMR, δ_H (300 MHz, 298 K, CD_3OD, standard TMS): 6.95 [2H, t, (J = 7 Hz)], 7.21 [2H, d, (J = 8.3 Hz)], 7.42 [2H, t, (J = 7 Hz)], 8.15 [2H, d, (J = 8.3 Hz)] and 9.17 (2H, s). FAB-MS (−ve): *m*/*z* 528 (M^-).

$[Os^{VI}(N)(HL^2)]$. was prepared in a manner similar to that of **7a**. Yield = 62 mg, 83%. Found: C, 38.8; H, 1.71; N, 6.78. $C_{20}H_{11}N_3O_4Cl_2Os$ requires C, 38.8; H, 1.79; N, 6.79%. IR (KBr, cm^{-1}): 2930, 1600 (CO) and 1460. NMR, δ_H (300 MHz, 298 K, CD_3OD, standard TMS): 6.91 [2H, t, (J = 8.21 Hz)], 7.2 [2H, d, (J = 7.51 Hz)], 7.38 [2H, d, (J = 8.2 Hz)], 7.51 [2H, d, (J = 7.51 Hz)] and 9.2 (2H, s). ESI-MS (−ve): *m*/*z* 617 (M^-).

$[Ru^{VI}(N)(HL^3)]$ [H_4L^3: 1,2-bis(2-hydroxybenzamido)-benzene]. Yield = 43 mg, 67%. Found: C, 52.2; H, 2.77; N, 9.12. $C_{20}H_{13}N_3O_4Cl_2Ru$ requires C, 52.2; H, 2.85; N, 9.13%. IR (KBr, cm^{-1}): 2945, 1603 (CO) and 1462. NMR, δ_H (300 MHz, 298 K, CD_3OD, standard TMS): 6.93 (2H, m), 6.99 (2H, m), 7.24 [2H, d, (J = 6.9 Hz)], 7.34 (2H, m), 8.15 [2H, dd, (J = 7.9 Hz, 1.6 Hz)] and 8.85 (2H, m). ESI-MS (−ve): *m*/*z* 459 (M^-).

$[Os^{VI}(N)(HL^3)]$. Yield = 44 mg, 67%. Found: C, 43.3; H, 2.33; N, 7.67. $C_{20}H_{13}N_3O_4Os$ requires C, 43.2; H, 2.38; N, 7.65%. IR (KBr, cm^{-1}): 2855, 1600 (CO), 1476 and 1195. NMR, δ_H (300 MHz, 298 K, CD_3OD, standard TMS): 6.95 (4H, m), 7.34 (4H, m), 8.31 [2H, d, (J = 7.8 Hz)] and 8.97 [2H, dd, (J = 6.3 Hz, 3.5 Hz)]. ESI-MS (−ve): *m*/*z* 548 (M^-).

[n-Bu_4N]$[Os^{VI}(N)(L^2O_2)]$ (8). A MeOH solution (15 cm^3) of [n-Bu_4N]$[Os^{VI}(N)(L^2)]$ (100 mg, 0.12 mmol) and $PhI(OAc)_2$ (112 mg, 0.35 mmol) was stirred for 3 h at room temperature, an orange solution was obtained. Excess Hpz (*ca.* 500 mg) was added to the reaction mixture, which was stirred for another 24 h. Removal of solvent by rotary evaporation gave an orange solid, which was dissolved in CH_2Cl_2 (1 cm^3) and loaded onto an alumina column (activity 90, neutral) for chromatographic purification using $CHCl_3$ as eluant. An orange band was collected and complete removal of solvent by rotary evaporation gave an orange solid. The crude product was recrystallized by diffusion of Et_2O to a CH_2Cl_2 solution to give orange crystals. Yield = 5 mg, 10%. Found: C, 48.5; H, 4.98; N, 6.52. $C_{36}H_{44}N_4O_6Cl_2Os$ requires C, 48.6; H, 4.98; N, 6.30%. IR (KBr, cm^{-1}): 2964, 2876, 1656 (CO), 1618, and 1096. NMR, δ_H (300 MHz, 298 K, CD_2Cl_2, standard TMS): 6.71 [2H, d, (J = 2.5 Hz)], 6.95–7.01 (1H, m), 7.28 [1H, d, (J = 8.1 Hz)], and 7.38–7.43 [1H, m, (J = 8.4 Hz)], 8.26 [1H, d, (J = 6.6 Hz)], 8.9 (1H, s) and 9.26 (1H, s). ESI-MS (−ve): *m*/*z* 648 (M^-).

Results and discussion

Reactions with phosphines

We previously reported that $[Ru^{VI}(L^1)(N)Cl]$ (**1**) reacted with PPh_3 in a CH_2Cl_2–py mixture to give $[Ru^{IV}(N{=}PPh_3)(L^1)(py)Cl]$ based on ^{31}P NMR and FAB-MS analyses. When the reaction mixture was left standing for > 14 h, $[Ru^{III}(L^1)(py)_3]^+$ complex was isolated (67 % yield) with the loss of the phosphiniminato group. In view of steric bulkiness of L^1 and PPh_3, we studied the "**1** + PPh_3" reaction for entry to coordinatively unsaturated bis(alkoxy)ruthenium complexes (Scheme 1).

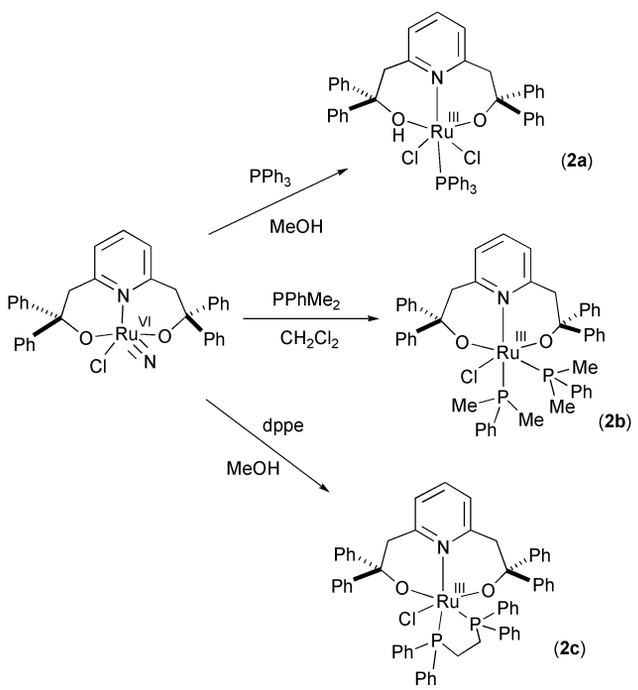

Scheme 1 Reactions with phosphines.

When **1** was treated with excess PPh_3 (10 equiv.) in degassed MeOH, $[Ru^{III}(HL^1)(PPh_3)Cl_2]$ (**2a**) was formed in 19% yield. Using 20 equiv. of PPh_3 afforded **2a** exclusively in similar yield, and any coordinatively unsaturated complexes such as $[Ru^{III}$-$(HL^1)(PPh_3)_2]$ were not obtained. Complex **2a** in CH_2Cl_2 exhibits an intense UV-VIS absorption band at λ_{max}/nm (ε/dm^3 mol^{-1} cm^{-1}) = 428 (1300), which is conspicuously absent in the UV-VIS spectrum of the starting complex. The $[Ru^{III}(HL^1)$-$(PPh_3)Cl_2]$ formulation is supported by FAB-MS [(*m*/*z* = 868 (M^+)] and elemental analysis. The ^1H NMR spectrum of **2a** is featured by broad absorption bands, indicative of paramagnetic nature of the complex.

The molecular structure of **2a** was established by X-ray crystallography. As shown in Fig. 2, the Ru atom adopts a distorted octahedral coordination. A notable feature is the unsymmetrical Ru–O distances. The Ru–O(1) distance is 1.974(3) Å, which is close to the corresponding distances of 1.902(3) and 1.921(3) Å in **1**. However, the Ru–O(2) distance [2.123(3) Å] is significantly longer than the Ru–O(1) distance. Compared to the Ru–OH_2 distances in both $[Ru^{II}(Me_3tacn)(bpy)(OH_2)]^{2+}$ [2.168(3) Å; Me_3tacn = trimethyl-1,4,7-triazacyclononane, bpy = 2,2′-bipyridine] [17] and $[Ru^{III}(N_2O_2)(OH)(OH_2)]^{2+}$ [2.199(3) Å; N_2O_2 = 1,12-dimethyl-3,4:9,10-dibenzo-1,12-diaza-5,8-dioxacyclopentadecane],[18] the Ru–O(2) value is comparable to a Ru–OH_2 distance, suggesting that O(2) is protonated. The PPh_3

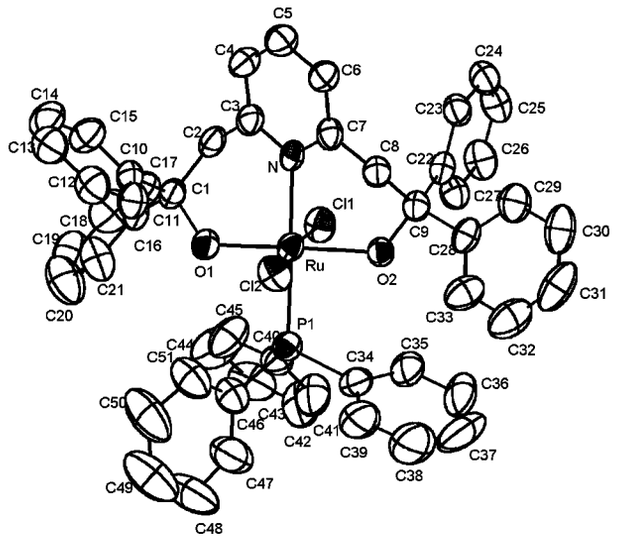

Fig. 2 Perspective view of $[Ru^{III}(HL^1)(PPh_3)Cl_2]$ (**2a**) with atom labelling scheme (50% probability ellipsoids).

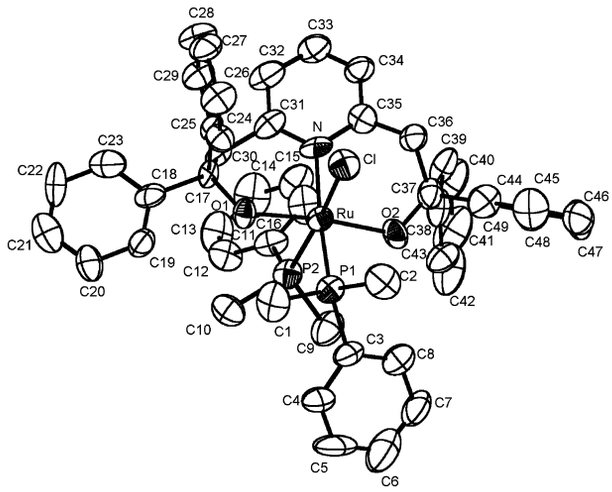

Fig. 3 Perspective view of $[Ru^{III}(L^1)(PPhMe_2)_2Cl]$ (**2b**) with atom labelling scheme (50% probability ellipsoids).

ligand is located *trans* to the pyridyl group with the Ru–P and Ru–N distances being 2.348(15) and 2.17(4) Å, respectively.

The failure to obtain coordinatively unsaturated complexes can be ascribed to steric repulsion between the bulky L^1 and PPh_3 ligands. This prompted us to employ $PPhMe_2$ as a less bulky phosphine derivative for the "**1** + phosphine" reaction. When **1** was treated with $PPhMe_2$ (3 equiv.) in degassed CH_2Cl_2, $[Ru^{III}(L^1)(PPhMe_2)_2Cl]$ (**2b**) was produced as a yellow solid in 83% yield. The molecular structure of **2b** is depicted in Fig. 3. The six-coordinated Ru atom adopts a distorted octahedral structure. Unlike **2a**, both the Ru–O distances [Ru–O(1) = 2.001(9) Å; Ru–O(2) = 2.008(9) Å] are comparable to the corresponding values [Ru–O(1) = 1.902(3) Å; Ru–O(2) = 1.921(3) Å] in **1**, suggesting that the O(1) and O(2) atoms remain in a deprotonated form. The two $PPhMe_2$ ligands are *cis*-coordinating to the Ru atom, and the Ru–P(1) distance [2.326(5) Å] is considerably shorter than the Ru–P(2) one [2.415(4) Å]. The difference in the Ru–P distances between the equatorial and axial coordinating $PPhMe_2$ ligands is discernible since the axial $PPhMe_2$ ligand would experience unfavorable steric interaction with the nearby phenyl groups (Fig. 3).

Analogous to **2b**, $[Ru^{III}(L^1)(dppe)Cl]$ (**2c**) was prepared by reacting **1** with excess dppe in MeOH. As expected, **2c** is structurally similar to **2b** based on crystallographic studies; the Ru–O(1) and Ru–O(2) distances are compatible with Ru–O(alkoxide) linkages. The Ru–P(1) and Ru–P(2) distances are 2.348(13) and 2.338(14) Å, respectively.

Reaction with amines

It is known that M≡N complexes would react with amines by nucleophilic addition. For example, Meyer[2e] and co-workers previously showed that the $[Os^{VI}(N)(terpy)Cl_2]^+$ complex [terpy = 2,2′,6′,2″-terpyridine] would react with morpholine and piperidine to form a hydrazido-osmium(IV) species. In this work, when **1** was treated with morpholine in CH_2Cl_2, only a gummy solid was obtained by Et_2O induced precipitation. Analysis of the solid by FAB-MS revealed two prominent ionic species at m/z = 672 and 656, which did not correspond to $[Ru^{VI}(N)(L^1)]^+$ (m/z = 584) or $[Ru^{III}(L^1)(C_4H_9NO)_2]^+$ (m/z = 744) species. Based on the agreement of the experimental and calculated isotopic patterns, the two species are designated to $[Ru^{III}(N)(L^1)(C_4H_9NO)]^+$ (m/z = 672) and $[Ru^{III}(L^1)(C_4H_9NO)]^+$ (m/z = 656) formulations. The expected ruthenium-hydrazido complex was not obtained.

Interestingly, we obtained $[Ru^{III}(L^1)(py)_2Cl]$ (**3a**) as a yellow crystalline solid (37% yield) when treating **1** with excess pyridine (py) [CH_2Cl_2 : py = 20 : 1 (v/v)]. Infra-red spectral analysis of **3a** revealed the absence of a Ru≡N stretch at 1000–1100 cm^{-1} (Ru≡N stretch for **1** is at 1025 cm^{-1}), indicative of the loss of the nitrido ligand after the reaction. The ^1H NMR spectrum featured broad resonances, suggesting a paramagnetic nature for the complex. By means of ESI-MS analysis, we observed a prominent ionic species with m/z = 650, which was assigned to a $[Ru^{III}(L^1)(py)]^+$ complex based on excellent agreement between the calculated and experimental isotopic distribution patterns (Scheme 2).

Likewise, **1** would react with pyrazole (Hpz) to furnish $[Ru^{III}(L^1)(Hpz)_3]Cl$ (**3b**) in 31% isolated yield. The molecular structures of **3a**–**b** have been established by X-ray crystallography (see later section).

In contrast to the analogous reaction of $[Os^{VI}(N)(terpy)Cl_2]^+$ complex, the reaction of **1** with morpholine is characterized by the loss of the nitrido ligand accompanied with ligand substitution. In this case, no hydrazido-ruthenium complex was obtained. For the less electrophilic osmium complexes, $[Os^{VI}(N)(L^1)Cl]$ reacted with morpholine and piperidine to give the adduct complexes $[Os^{VI}(N)(L^1)Cl(morpholine)]$ and $[Os^{VI}(N)(L^1)Cl(piperidine)]$, which have been structurally characterized by X-ray crystallography.

The molecular structure of $[Ru^{III}(L^1)(py)_2Cl]$ (**3a**) is depicted in Fig. 4. As shown in the figure, the ruthenium atom adopts a distorted octahedral coordination geometry. The two measured Ru–O(1) [1.999(3) Å] and Ru–O(2) [1.987(4) Å] distances are comparable to the corresponding distances for $[Ru^{III}(L^1)(dppe)Cl]$ [Ru–O(1) = 1.999(3) and Ru–O(2) = 1.987(4) Å]. This finding suggests that the coordinated L^1 ligand is in a doubly

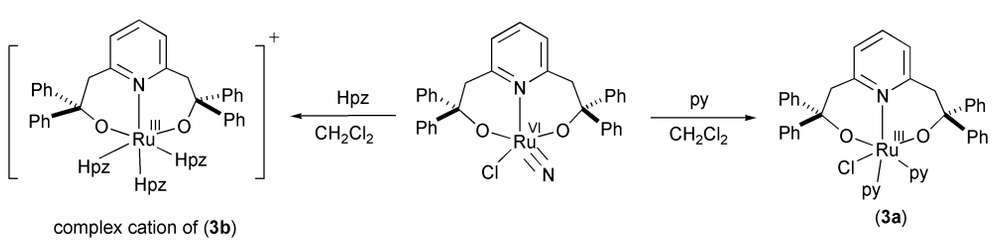

Scheme 2 Reactions in the py–CH_2Cl_2 and Hpz–CH_2Cl_2 solutions.

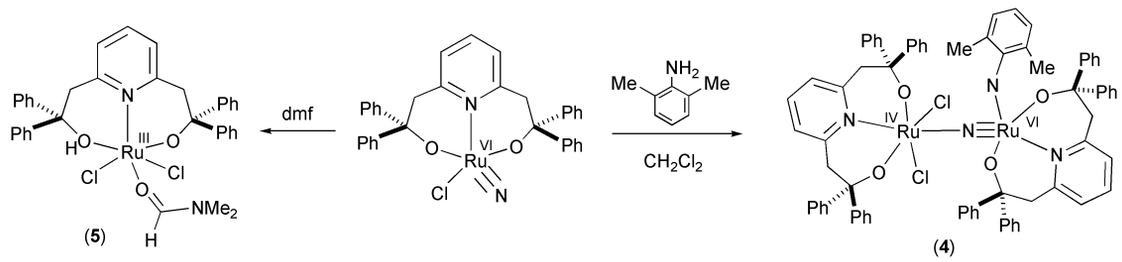

Scheme 3 Reactions with 2,6-dimethylaniline and dimethylformamide.

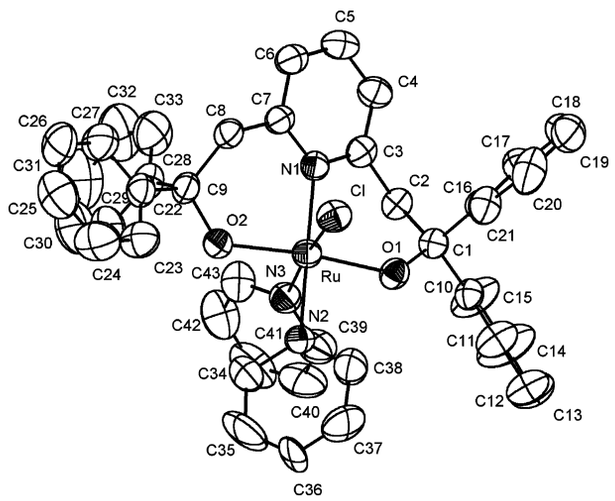

Fig. 4 Perspective view of $[Ru^{III}(L^1)(py)_2Cl]$ (**3a**) with atom labelling scheme (50% probability ellipsoids).

deprotonated form (*i.e.*, bis-alkoxides). The Ru, O(1), C(1), C(2), C(3) and N(1) atoms, as well as the Ru, O(2), C(9), C(8), C(7) and N(1) atoms, constitute a pair of six-membered rings; both of them adopt a boat conformation. The two pyridine ligands are *cis*-coordinating and the Ru–N(2) and Ru–N(3) bond distances [Ru–N(2) = 2.103(4) and Ru–N(3) = 2.126(4) Å] are comparable to the corresponding values in $[Ru(bpy)_2(py)_2][(+)$-*O*,*O*′-dibenzoyl-D-tartrate] [Ru–N(41) = 2.114(5) and Ru–N(31) = 2.122(5) Å].[19]

Analogous to **3a**, $[Ru^{III}(L^1)(Hpz)_3]Cl$ (**3b**) has a similar molecular structure (Fig. 5). The six-coordinated ruthenium atom is bound to L^1 and the three Hpz molecules are arranged in a meridional configuration. The O(1)–Ru–O(2) angle is 169.94(12)°, which is close to the corresponding angle of 173.3(1)° in $[Ru^{III}(L^1)(py)_2Cl]$. The three Ru–N (Hpz) distances of 2.073(4), 2.086(4) and 2.089(3) Å are similar.

We have also examined the reactions of **1** with aromatic amines such as aniline, which is a weaker nucleophile compared to morpholine. When **1** was reacted with 2,6-dimethylaniline (DMA; 3 equiv.) in CH_2Cl_2, the red-brown $[Ru^{IV}(L^1)Cl_2(\mu\text{-}N)Ru^{VI}(L^1)(C_8H_{10}N)Cl]$ complex (**4**) was produced in 10% yield (Scheme 3). Based on X-ray crystallographic studies, **4** was found to be a dinuclear μ-nitridoruthenium complex as depicted in Fig. 6. The structure is characterized by an unsymmetrical linear Ru(1)–N(1)–Ru(2) configuration [170.7(3)°]; the measured Ru(1)–N(1) and Ru(2)–N(1) distances are 1.661(5) and 1.837(5) Å, respectively. The short Ru(1)–N(1) distance is characteristic of a Ru≡N bond, which is slightly longer than the corresponding distance of 1.605(4) Å in **1**. Compared to a Ru–N single bond (*ca.* 2.0–2.1 Å), the Ru(2)–N(1) distance [1.837(5) Å] is apparently shorter, suggesting multiple bonding character. Therefore, coordination of Ru(2) atom to Ru(1)≡N(1) causes delocalization of some π-electron density to the Ru(2)–N(1) bond, leading to weakening of the Ru(1)≡N(1) linkage.

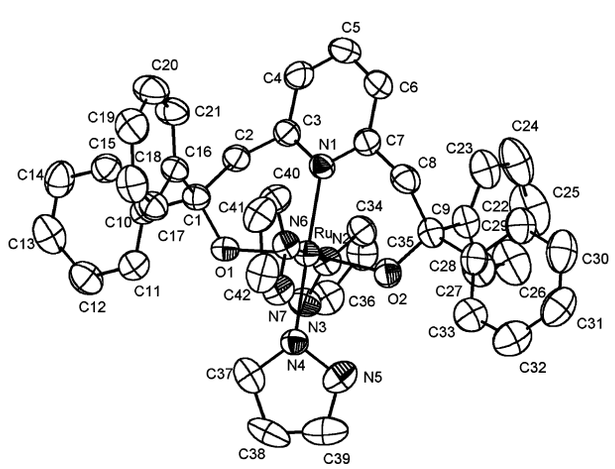

Fig. 5 Perspective view of the complex cation of $[Ru^{III}(L^1)(Hpz)_3]$-Cl (**3b**) with atom labelling scheme (50% probability ellipsoids).

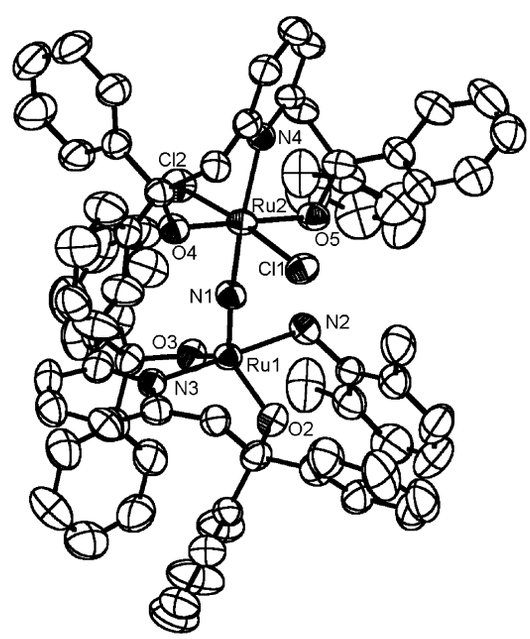

Fig. 6 Perspective view of $[Ru^{IV}(L^1)Cl_2(\mu\text{-}N)Ru^{VI}(L^1)(C_8H_{10}N)Cl]$ (**4**) with atom labelling scheme (50% probability ellipsoids). The atom labelling for non-esssential bonding atoms is omitted for clarity.

Notably, the dinuclear complex is constituted by two structurally distinct Ru fragments, which exhibit different coordination geometries. The five-coordinated Ru(1) atom exhibits a distorted trigonal bipyrimidal configuration, which is isostructural to the starting ruthenium complex **1**. The N(2)–Ru(1)–N(3) axis [177.15(17)°] is close to linearity, and the trigonal plane is defined by the Ru(1), N(1), O(2) and O(3) atoms. The respective Ru(1)–O(2) and Ru(1)–O(3) distances are 1.906(5) and 1.919(4) Å, which are close to the corresponding distances of [Ru–O(1) = 1.902(3) Å; Ru–O(2) = 1.921(3) Å] in **1**. The respective Ru(1)–N(2) and Ru(1)–N(3) distances are 2.175(5) and 2.077(5) Å, which are compatible with a Ru–N single bond distance.

The six-coordinated Ru(2) atom adopts a distorted octahedral configuration. The N(1)–Ru(2)–N(4) [175.4(2)°], O(4)–Ru(2)–O(5) [178.59(16)°] and Cl(11)–Ru(2)–Cl(12) axes [174.36(7)°] are close to linearity, and the Ru(2)–O(4) [1.943(4) Å] and Ru(2)–O(5) [2.003(4) Å] distances are comparable to the corresponding distances in **1**.

Analogous to the reactions with amines and anilines, **1** was found to be transformed to $[Ru^{III}(HL^1)(dmf)Cl_2]$ (**5**) in a dmf (10 cm^3) solution. Complex **5** was isolated as a red-brown solid in 17% yield. The IR spectrum of **5** revealed the absence of Ru≡N stretch, and there are two intense absorptions at 1639 and 1655 cm^{-1} characteristic of C=O stretches of the co-ordinated and free dmf molecules, respectively. The FAB-MS spectrum is featured by a prominent ion peak at a m/z = 606 assignable to a $[Ru^{III}(HL^1)Cl]^+$ species. The ^1H NMR spectrum shows broad signals revealing that the complex is paramagnetic. In CH_2Cl_2, the complex shows several intense UV-VIS absorption bands at λ_{max}/nm (ε/dm^3 mol^{-1} cm^{-1}) at 266 (br, 10000), 330 (sh, 3400), and 420 (sh, 2050). The 420 nm band is tentatively assigned to a $p_\pi(Cl^-) \longrightarrow Ru(III)$ charge transfer transition.

The molecular structure of **5** has been determined by X-ray crystal analysis. As depicted in Fig. 7, the ruthenium atom co-ordinates to the tridendate L^1, the dmf and the two *trans*-chloro ligands, which together adopt a distorted octahedral geometry. The Ru–N(1) distance of 2.073(3) Å is close to the corresponding distances [2.085(5)–2.141(5) Å] found in **1** and some $[Ru^{III}(N_4)Cl_2]^+$ complexes (N_4 = macrocyclic tertiary amines).[20] The two Ru–O distances are unsymmetrical with Ru–O(1) and Ru–O(2) distances being 2.127(2) and 1.927(2) Å, respectively. The differential Ru–O distances suggests that L^1 is in a mono-protonated form. The respective Ru–Cl(1) and Ru–Cl(2) distances are 2.384 (1) and 2.38(1) Å. The dmf molecule co-ordinates to the Ru atom through the carbonyl oxygen atom with a Ru–O(3)–C(34) angle of 120.7(2)°; a similar coordination mode for dmf can be found in $[Ru^{II}(dmf)_6](CF_3SO_3)_2$ (Ru–O=$C_{average}$ 121.75°)].[21] The C(34)–O(3) [1.234(4) Å] and C(34)–N(2) [1.298(5) Å] distances of the coordinated dmf are comparable to the corresponding values found in $[Ru^{II}(dmf)_6](CF_3SO_3)_2$.

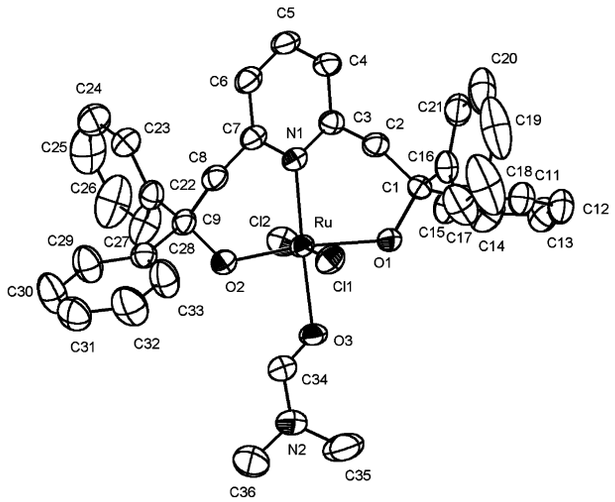

Fig. 7 Perspective view of $[Ru^{III}(HL^1)(dmf)Cl_2]$ (**5**) with atom labelling scheme (50% probability ellipsoids).

Electrophilic attack on metal-nitrido complex

Reactions of nitrido ligand in late transition metal-nitrido complexes toward electrophilies are sparse in the literature.[22] In contrast, the nitrido ligand in some early transition metal-nitrido complexes [*e.g.* $[Mo(N)(S_2CNR_2)_3]$ and *trans*-$[Mo(N)X(dppe)_2]$[23] and $[Re(N)Y_2(PEt_2Ph)_3]$[24] (Y = Cl and Br)] are known to react with electrophilies such as H^+, $(Me_3O)BF_4$ and BX_3 (X = F, Cl, Br). Previously, Shapley and co-workers reported that a series of Os(VI) nitrido-alkyl complexes, $[n\text{-}Bu_4N][Os^{VI}(N)R_4]$ (R = Me, CH_2SiMe_3, CH_2CMe_3 and CH_2Ph_2), reacts with $(Me_3O)BF_4$ by electrophilic alkylation of the nitrido ligand to generate imido-osmium(VI) complexes.[25]

In this work, we are interested to explore the reactivity of nitridoruthenium(VI) complexes toward electrophilic reagents (Scheme 4). When **1** was treated with excess $(Me_3O)BF_4$ in CH_2Cl_2, a red crystalline solid was isolated and characterized by X-ray crystal analysis to be $[Ru^{VI}_2(N)_2(L^1)_2(OH)]PF_6$ (**6**), which contains two Ru≡N groups and the two ruthenium atoms are bridged by a hydroxyl group.

The IR spectrum of **6** shows an absorption band at 3498 cm^{-1}, assignable to a ν_{OH} stretch. The Ru≡N stretch could not be located because of extensive overlapping peaks due to the ligand absorptions at the 1200–800 cm^{-1} region. As **6** is diamagnetic, the bridging hydroxyl proton can also be found in the ^1H NMR spectrum (δ_H = 10.0 ppm).

As shown in Scheme 5 the formation of **6** was believed to be initiated by electrophilic attack of a "CH_3^+" cation on the chloride ligand, followed by the loss of CH_3Cl and generation of a coordinately unsaturated $[Ru{\equiv}N]^+$ species. A similar

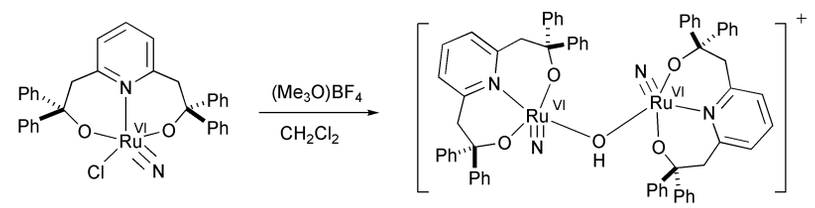

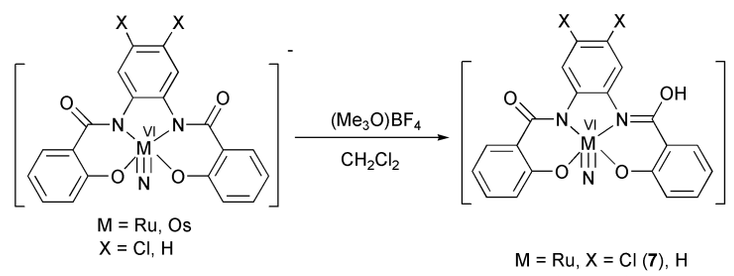

Scheme 4 Reaction with trimethyloxonium tetrafluoroborate.

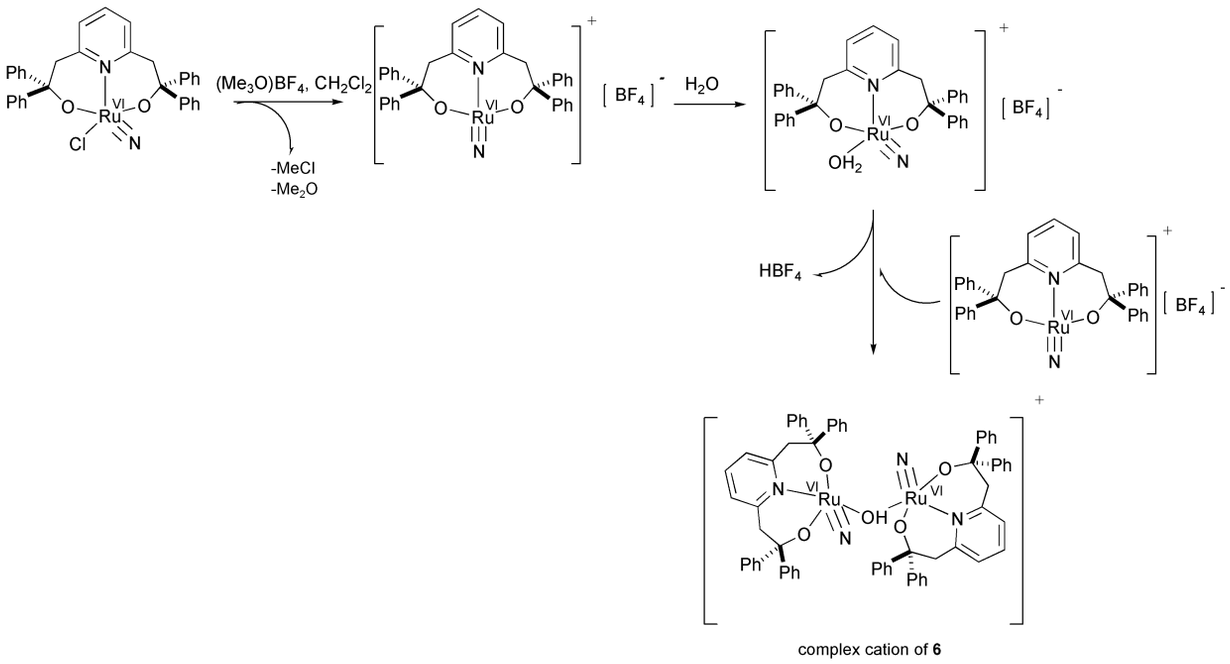

Scheme 5 Proposed reaction sequence for the formation of **6**.

reaction was reported earlier by Shapley and co-workers showing that nitridoruthenium(VI) alkyl complexes readily underwent dealkylation in the presence of HCl.[26] The vacant site would be taken up by a H_2O molecule; the μ-OH complex was formed upon reaction with another molecule of coordinatively unsaturated $[Ru{\equiv}N]^+$ species. It should be noted that treatment of **1** with silver trifluoromethanesulfonate in acetone or acetonitrile in room temperature did not give AgCl.

It is widely believed that oxidation of cationic ruthenium-amine complexes would proceed through a highly reactive nitridoruthenium intermediate, which reacts with water to give a nitrosyl-ruthenium complex as the isolated product.[27] Examples of structurally characterized cationic nitridoruthenium complexes are sparse in the literature. In 1995, we reported the first structurally characterized nitridoruthenium complex, $[(Ru^{VI}(N)(heda)_2)_2(\mu\text{-}O)]ClO_4$ (heda = 2,5-dimethyl-2,5-hexanediamine).[28]

Fig. 8 depicts the molecular structure of $[Ru^{VI}(N)(L^1)(\mu\text{-}OH)\text{-}Ru^{VI}(N)(L^1)]^+$, which represents the second example of structurally defined cationic nitridoruthenium complexes. As shown in the figure, the two Ru≡N moieties are connected through a bridging OH ligand, and the N(1)–Ru(1)–O(1) and N(2)–Ru(2)–O(1) angles are 100.1(2) and 100.6(2)°, respectively. The coordination geometries of the ruthenium atoms are similar to that of **1**. The Ru≡N distances are 1.603(4) Å [Ru(1)–N(1)] and 1.613(4) Å [Ru(2)–N(2)], which are similar to the corresponding distance of [Ru(1)–N(1) = 1.615(4) Å] in **1.** Yet, the observed Ru≡N distances in **6** are substantially shorter than 1.66(1) Å found in the related $[(Ru^{VI}(N)(heda)_2)_2(\mu\text{-}O)]ClO_4$ complex.[28] Each Ru complex fragment can be described as a distorted trigonal bipyramid, and the N(1), O(2), O(3) and N(2), O(4), O(5) atoms are situated on two distorted trigonal planes. Structurally analogous to **1**, the O(1)–Ru(1)–N(3) [164.94(12)°] and O(1)–Ru(2)–N(4) [163.79(12)°] axes deviate significantly from linearity. The two trigonal planes defined by the Ru(1), N(1), O(2), O(3) and Ru(2), N(2), O(4), O(5) atoms are nearly isosceles triangles. The respective Ru(1)–O(2), Ru(1)–O(3), Ru(2)–O(4) and Ru(2)–O(5) distances are 1.934(3), 1.928(3), 1.93(3), and 1.923(3) Å, which are typical values of a Ru–O single bond formulation. The Ru(1)–O(1)–Ru(2) moiety in **6** is not linear with an angle of 136(1)°, unlike the corresponding bond angle [180(2)°] in $[(Ru^{VI}(N)(heda)_2)_2(\mu\text{-}O)]ClO_4$.[28]

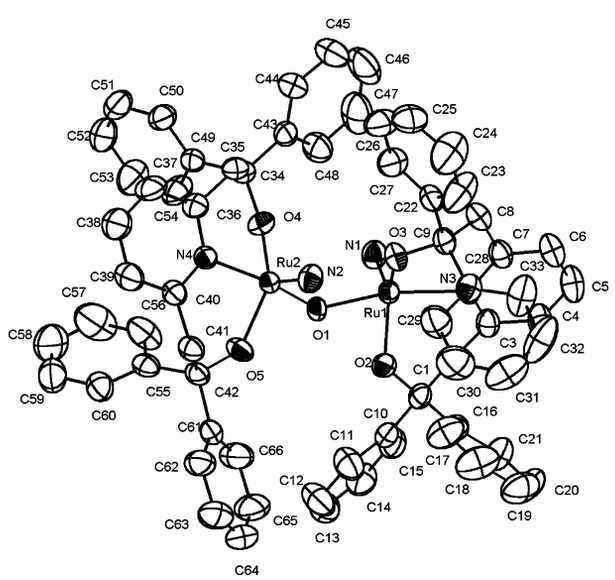

Fig. 8 Perspective view of the complex cation of $[Ru^{VI}_2(N)_2(L^1)_2\text{-}(OH)]PF_6$ (**6**) with atom labelling scheme (50% probability ellipsoids).

It has been documented that electrophilic alkylation (*N vs. S*-alkylation) of $[n\text{-}Bu_4N][Os(NCPh_3)(S_2C_6H_4)_2]$ can preferentially take place at the nitrido ligand by employing encumbered electrophilic reagents such as $(Ph_3C)PF_6$.[29] However, when $[Ru^{VI}(N)(L^1)Cl]$ (**1**) was treated with an excess of $(Ph_3C)PF_6$ in CH_2Cl_2, the dimeric nitrido complex **6** was formed exclusively, albeit in lower yield (30%). No *N*-alkylated nitridoruthenium complex was obtained.

Reports from various groups showed that nitrido-manganese(V)-porphyrins and -Schiff base complexes can effect alkene aziridination in the presence of trifluoroacetic anhydride and pyridine. A highly reactive *N*-trifluoroacetylimido-manganese species has widely been invoked as the active intermediate in such reactions.[10,11,30] In this work, reaction of $[Ru^{VI}(N)(L^1)Cl]$ with $(CF_3CO)_2O$ (3 equiv.)/cyclooctene (excess) in CH_2Cl_2 under an argon atmosphere did not afford any aziridine products. However, $[Ru^{VI}_2(N)_2(L^1)_2(\mu\text{-}OH)]PF_6$ was isolated in less than 10% yield. We postulate that the acid anhydride would attack the alkoxide oxygen atom resulting in extensive demetallation.

Similarly we proceeded to examine the reactions of $[n\text{-}Bu_4N][Ru^{VI}(N)(L^2)]$ toward electrophilic reagents under

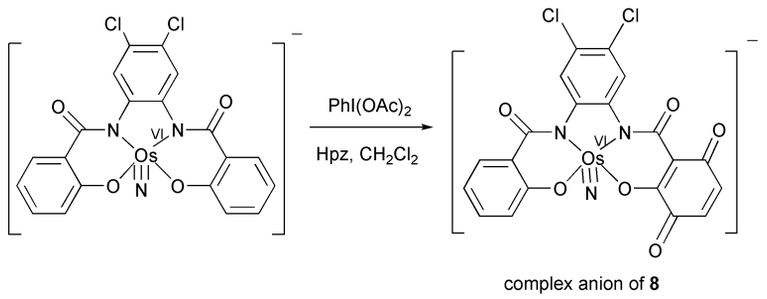

Scheme 6 Oxidation by iodosylbenzene diacetate.

similar conditions. Again, treating [n-Bu_4N][$Ru^{VI}(N)(L^2)$] with $(Me_3O)BF_4$ in CH_2Cl_2 did not result in *N*-alkylation. However, [n-Bu_4N][$Ru^{VI}(N)(L^2)$] underwent protonation at the C=O group of the ligand to form [$Ru^{VI}(N)(HL^2)$] (**7**), which was isolated as a yellow precipitate (>90% yield) (Scheme 6). Similar observation was obtained when HBF_4 was used as the electrophilic reagent. The ^1H and ^{13}C NMR spectra of the yellow product revealed identical spectral features as that of the starting nitridoruthenium(VI) complexes, except that the signals corresponding to the [n-Bu_4N]$^+$ protons were completely absent. Moreover, the ^1H NMR spectrum did not show any extra resonance corresponding to a methylimido (Ru≡NMe) moiety, nor any methoxy group arising from O-alkylation of the ligand. The IR and Raman spectra showed a sharp and strong absorption at 3125 cm^{-1}, which could either be a N–H or O–H stretch. This absorption is conspicuously absent in the corresponding spectrum of the starting complex.

The molecular structure of **7** was determined by X-ray crystallography (Fig. 9). The complex is isostructural to [$Ru^{VI}(N)(L^2)$]$^-$ with similar Ru≡N distance of 1.599(4) Å (*cf.* 1.609(6) Å for [n-Bu_4N][$Ru^{VI}(N)(L^2)$]). By careful inspection of the difference Fourier map, we did not find significant electron density that can be attributed to a H atom in the vicinity of the N^{3-} ligand. Therefore, *N*-protonation is unlikely. The coordination geometry of [$Ru^{VI}(N)(HL^2)$] (**7**) at the ruthenium atom is a distorted square pyramid, with the nitrido ligand at the apical position. The Ru atom is slightly lifted out of the mean plane defined by O(1), O(2), N(2) and N(3) by ~ 0.57 Å. The Ru–N(2), Ru–N(3), Ru–O(1) and Ru–O(2), distances are 2.029(4), 1.988(3), 1.964(3) and 1.975(3) Å, respectively. However, it is noteworthy that the auxiliary L^2 ligand displays a structural asymmetry in the C=O distance, *i.e.*, the O(3)–C(7) distance [1.296(5) Å] is significantly longer than the O(4)–C(14) distance [1.210(6) Å]. A similar differential in bond distances was observed for the amide groups, *i.e.*, N(2)–C(7) [1.326(5) Å] bond distance is close to a N=C bond length (*ca.* 1.31 Å in [Os^{IV}(salch-^{t}Bu)Cl_2][31] [salch-^{t}Bu = *trans*-1,2-bis(di-*tert*-butylsalicyliminato)cyclohexane]), whereas the N(3)–C(14) has a distance of 1.395(6) Å compatible with an amide bond (*cf.* 1.391 Å in [n-Bu_4N][$Ru^{VI}(N)(L^2)$]). Moreover, the O(3)–C(7) distance [1.296(5) Å] is significantly longer than the O(4)–C(14) distance [1.210(6)Å], which is a typical C=O double bond (*cf.* average 1.22 Å in [n-Bu_4N][$Ru^{VI}(N)(L^2)$]). In the literature, amide-to-iminol tautomerism is known,[32] for example, [Co(η^4-bpb)(η^2-Hbpb)][33] has two different C–N bonds [1.332(8) and 1.408(8) Å] assignable to an imine (C=N) and an amide [–C(=O)–N] linkage, respectively.

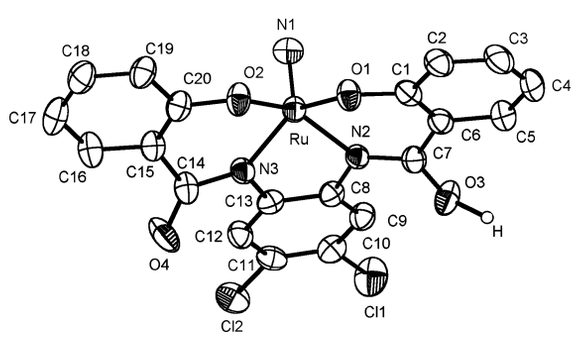

Fig. 9 Perspective view of [$Ru^{VI}(N)(HL^2)$] (**7**) with atom labelling scheme (50% probability ellipsoids).

The hydroxyl proton was located in the difference Fourier map and its positional parameters were included in the least squares refinement. The O(3)–H bond distance is 1.18 Å; the C(7)–O(3)–H angle is estimated to be 116.7°.

Similarly, $(Me_3O)BF_4$ reacted with [n-Bu_4N][$Ru^{VI}(N)(L^3)$], [n-Bu_4N][$Os^{VI}(N)(L^2)$], and [n-Bu_4N][$Os^{VI}(N)(L^3)$] to afford the ligand-protonated nitrido-metal complexes which have been characterized by spectroscopic means. The slow hydrolysis of $(Me_3O)BF_4$ due to moisture in CH_2Cl_2 would produce HBF_4, which would protonate the carbonyl group of the auxiliary ligand.

Oxidation by $PhI(OAc)_2$

Reactions of the nitrido-metal complexes with $PhI(OAc)_2$ (iodosylbenzene diacetate) have been examined. In MeOH, [n-Bu_4N][$Os^{VI}(N)(L^2)$] was found to undergo ligand-oxidation upon treatment with $PhI(OAc)_2$ (3 equiv.) in the presence of Hpz (10 equiv.) to give [n-Bu_4N][$Os^{VI}(N)(L^2O_2)$] (**8**), which was isolated as an orange crystalline solid in <10% yield after chromatographic purification (Scheme 6). Complex **8** was analyzed by ESI-MS, and a prominent ion cluster peak at *m*/*z* = 648 was observed. Based on the agreement of the experimental and calculated isotopic distribution patterns, an oxygenated derivative of [$Os^{VI}(N)(L^2)$]$^-$, *i.e.*, [$Os^{VI}(N)(L^2O_2)$]$^-$, was formulated. The IR spectrum of **8** revealed an intense absorption band at 1656 cm^{-1} characteristic of a C=O stretch, along with all the major spectral features of the starting complex. The UV-VIS absorption spectrum recorded in CH_2Cl_2 shows two intense absorption bands at λ_{max}/nm (ε/dm^3 mol^{-1} cm^{-1}) = 245 (49000) and 305 (23500) presumably due to intraligand transitions.

With regard to the low product yield, most of the starting complex (*ca.* 70%) was recovered during Et_2O induced crystallization. Analysis of the residual mother liquor by ESI-MS revealed several ion species with molecular ion peaks at *m*/*z* = 738, 716, 686, 678 and 604, which can be assigned to [Os^{IV}-(L^2)(Hpz)(pz)]$^-$, [$Os^{VI}(N)(L^2O_2)$(Hpz)]$^-$, [$Os^{VI}(N)(L^2)$ (Hpz)]$^-$, [$Os^{VI}(N)(L^2)$(AcOH)]$^-$ and [$Os^{III}(L^2)$]$^-$, respectively, based on the agreement of the experimental and calculated isotopic distribution patterns.

The molecular structure of **8** has been established by X-ray crystallography and is depicted in Fig. 10. One of the phenoxy moieties was oxygenated to give a 1,4-benzoquinone structure, whereas the Os≡N moiety [1.625(9) Å] remained unchanged after the reaction. The osmium atom adopts distorted square pyramidal coordination, isostructural to the starting complex [$Os^{VI}(N)(L^2)$]$^-$. For the benzoquinone moiety, the C(16)–O(5) and C(19)–O(6) bond distances are 1.223(13) and 1.252(14) Å, which is a typical C=O double bond [*cf.* average 1.22 Å] in [n-Bu_4N][$Os^{VI}(N)(L^2)$]. Moreover, the C(14)–C(15) [1.350(16) Å] and C(17)–C(18) [1.350(17) Å] distances are slightly shorter

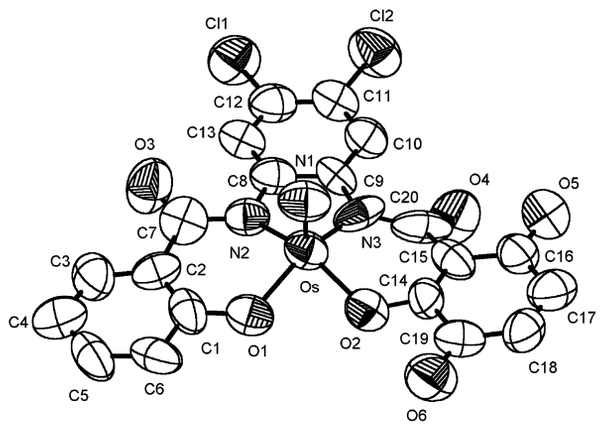

Fig. 10 Perspective view of the complex anion of $[n\text{-}Bu_4N][Os^{VI}(N)(L^2)O_2)]$ (**8**) with atom labelling scheme (50% probability ellipsoids).

than the corresponding bond distances in $[Os^{VI}(N)(L^2)]^-$ [1.386(11) Å], indicative of a C=C bond character. The C(15)–C(16) [1.446(16) Å], C(16)–C(17) [1.463(17) Å], C(18)–C(19) [1.438(18) Å] and C(14)–C(19) [1.522(16) Å] distances are compatible with a C–C single bond distance.

For the "$[n\text{-}Bu_4N][Os^{VI}(N)(L^2)]$+ $PhI(OAc)_2$" reaction, water is required for the formation of **8**. When dry CH_2Cl_2 or CH_3CN was employed as solvent, only the starting complex was recovered. In addition, when the reaction was carried out in the absence of Hpz as additive, only the starting complex was recovered (yield ~90%) and no **8** was obtained. Other oxidants such as iodosylbenzene and nitrosonium hexafluorophosphate are not effective for the oxidation of $[n\text{-}Bu_4N][Os^{VI}(N)(L^2)]$, and the starting complex was recovered.

However, the analogous reaction of $[n\text{-}Bu_4N][Os^{VI}(N)L^3]$ with $PhI(OAc)_2$ failed to afford the $[Os^{VI}(N)(L^3O_2)]^-$ complex in isolable quantity. However, analysis of the reaction mixture by ESI-MS revealed the product $[Os^{VI}(N)(L^3O_2)]^-$, characterized by the close agreement between the observed isotopic distribution pattern centered at m/z = 580 with that of proposed formulation.

In contrast, $[n\text{-}Bu_4N][Ru^{VI}(N)L^2]$ and $[n\text{-}Bu_4N][Ru^{VI}(N)L^3]$ were found to be inactive toward $PhI(OAc)_2$, and only the starting complexes were recovered after the reaction.

Conclusion

In this work, we examined a series of nucleophilic and electrophilic additions and oxidative reactions of some nitrido-ruthenium(VI) and -osmium(VI) complexes containing di- and tetra-anionic ligands. The high-valent nitrido-ruthenium(VI) complexes could be rather more electrophilic and reactive than their osmium analogues and the nitride (N^{3-}) ligand of the ruthenium dianionic complex is easily eliminated in the presence of nucleophiles. Also, we found that the metal-nitrido complexes are unreactive toward electrophiles. Interestingly, the $[n\text{-}Bu_4N][Os^{VI}(N)(L^2)]$ complex was found to undergo ligand oxidation with phenoxy group being transformed to a benzoquinone group.

Acknowledgements

This work is supported by the Areas of Excellence Scheme established under the University Grants Committee of the Hong Kong Special Administrative Region, China (Project AoE/P-10/01), The University of Hong Kong (University Development Fund) and the Hong Kong Research Grants Council (HKU7099/00P). We thank Prof. S.-M. Peng (National Taiwan University) and Dr. K.-K. Cheung for solving the crystal structures of **2b**, **6** and **7**.

References

1 (*a*) K. Dehnicke, F. Weller and J. Strähle, *Chem. Soc. Rev.*, 2001, **30**, 125; (*b*) K. Dehnicke and J. Strähle, *Angew. Chem., Int. Ed. Engl*, 1981, **20**, 413.
2 (*a*) M. H. V. Huynh, R. T. Baker, D. L. Jameson, A. Labouriau and T. J. Meyer, *J. Am. Chem. Soc.*, 2002, **124**, 4580; (*b*) M. H. V. Huynh, P. S. White and T. J. Meyer, *J. Am. Chem. Soc.*, 2001, **123**, 9170; (*c*) M. H. V. Huynh, P. S. White, C. A. Carter and T. J. Meyer, *Angew. Chem., Int. Ed.*, 2001, **40**, 3037; (*d*) M. H. V. Huynh, P. S. White, K. D. John and T. J. Meyer, *Angew. Chem., Int. Ed.*, 2001, **40**, 4049; (*e*) M. H. V. Huynh, D. L. Jameson and T. J. Meyer, *Inorg. Chem.*, 2001, **40**, 5062–5063; (*f*) M. H. V. Huynh, E.-S. El-Samanody, K. D. Demadis, T. J. Meyer and P. S. White, *J. Am. Chem. Soc.*, 1999, **121**, 1403.
3 (*a*) T. J. Crevier, B. K. Bennett, J. D. Soper, J. A. Bowman, A. Dehestani, D. A. Hrovat, S. Lovell, W. Kaminsky and J. M. Mayer, *J. Am. Chem. Soc.*, 2001, **123**, 1059; (*b*) B. K. Bennett, S. Lovell and J. M. Mayer, *J. Am. Chem. Soc.*, 2001, **123**, 4336; (*c*) B. K. Bennett, S. J. Pitteri, L. Pilobello, S. Lovell, W. Kaminsky and J. M. Mayer, *J. Chem. Soc., Dalton Trans.*, 2001, 3489; (*d*) M. R. McCarthy, T. J. Crevier, B. Bennett, A. Dehestani and J. M. Mayer, *J. Am. Chem. Soc.*, 2000, **122**, 12391; (*e*) T. J. Crevier and J. M. Mayer, *J. Am. Chem. Soc.*, 1998, **120**, 5595; (*f*) T. J. Crevier, S. Lovell and J. M. Mayer, *J. Am. Chem. Soc.*, 1998, **120**, 6607.
4 (*a*) S.-M. Chiu, T.-W. Wong, W.-L. Man, W.-T. Wong, S.-M. Peng and T.-C. Lau, *J. Am. Chem. Soc.*, 2001, **123**, 12720–12721; (*b*) T.-W. Wong, T.-C. Lau and W.-T. Wong, *Inorg. Chem.*, 1999, **38**, 6181–6186.
5 (*a*) M. H. V. Huynh, D. E. Morris, P. S. White and T. J. Meyer, *Angew. Chem., Int. Ed.*, 2002, **41**, 2330; (*b*) M. H. V. Huynh, P. S. White and T. J. Meyer, *Inorg. Chem.*, 2001, **40**, 5231; (*c*) M. H. V. Huynh, E.-S. El-Samanody, K. D. Demadis, P. S. White and T. J. Meyer, *Inorg. Chem.*, 2000, **39**, 3075; (*d*) M. H. V. Huynh, T. J. Meyer and P. S. White, *J. Am. Chem. Soc.*, 1999, **121**, 4530; (*e*) D. W. Pipes, M. Bakir, S. E. Vitols, D. J. Hodgson and T. J. Meyer, *J. Am. Chem. Soc.*, 1990, **112**, 5507.
6 J. D. Soper, B. K. Bennett, S. Lovell and J. M. Mayer, *Inorg. Chem.*, 2001, **40**, 1888.
7 (*a*) K.-F. Chin, K.-K. Cheung, H.-K. Yip, T. C.-W. Mak and C.-M. Che, *J. Chem. Soc., Dalton Trans.*, 1995, 657; (*b*) C.-M. Che, K.-Y. Wong, H.-W. Lam, K.-F. Chin, Z.-Y. Zhou and T. C.-W. Mak, *J. Chem. Soc., Dalton Trans.*, 1993, 857; (*c*) H.-W. Lam, C.-M. Che and K.-Y. Wong, *J. Chem. Soc., Dalton Trans.*, 1992, 1411; (*d*) C.-M. Che, T.-C. Lau, H.-W. Lam and C.-K. Poon, *J. Chem. Soc., Chem. Commun.*, 1989, 114.
8 S. B. Seymore and S. N. Brown, *Inorg. Chem.*, 2002, **41**, 462.
9 K. D. Demadis, T. J. Meyer and P. S. White, *Inorg. Chem.*, 1997, **36**, 5678.
10 J. T. Groves and T. Takahashi, *J. Am. Chem. Soc.*, 1983, **105**, 2073.
11 J. Du Bois, C. S. Tomooka, J. Hong and E. M. Carreira, *Acc. Chem. Res.*, 1997, **30**, 364.
12 (*a*) C.-M. Che and V. W.-W. Yam, *Adv. Inorg. Chem.*, 1992, **39**, 233–325; (*b*) V. W.-W. Yam and C.-M. Che, *Coord. Chem. Rev.*, 1990, **97**, 93.
13 S. K.-Y. Leung, J.-S. Huang, J.-L. Liang, C.-M. Che and Z.-Y. Zhou, *Angew. Chem., Int. Ed.*, 2003, **42**, 340.
14 (*a*) L. Bonomo, E. Solari, R. Scopelliti and C. Floriani, *Angew. Chem., Int. Ed.*, 2001, **40**, 2529; (*b*) P.-M. Chan, W.-Y. Yu, C.-M. Che and K.-K. Cheung, *J. Chem. Soc., Dalton Trans.*, 1998, 3183; (*c*) D. Sellmann, M. W. Wemple, W. Donaubauer and F. W. Heinemann, *Inorg. Chem.*, 1997, **36**, 1397; (*d*) J. J. Schwab, E. C. Wilkinson, S. R. Wilson and P. A. Shapley, *J. Am. Chem. Soc.*, 1991, **113**, 6124.
15 P. T. Beurskens, G. Admiraal, G. Beuskens, W. P. Bosman, S. Gercia-Granda, R. O. Gould, J. M. M. Smith and C. Smyklla, *The DIRDIF program system*, Technical Report of the Crystallography Laboratory, University of Nijmegen, The Netherlands, 1992.
16 TEXSAN Crystal Structure Analysis Package, Molecular Structure Corporation, Houston, TX, 1985 and 1992.
17 W.-C. Cheng, W.-Y. Yu, K.-K. Cheung and C.-M. Che, *J. Chem. Soc., Dalton Trans.*, 1994, 57.
18 C.-M. Che, W.-T. Tang, W.-T. Wong and T.-F. Lai, *J. Am. Chem. Soc.*, 1989, **111**, 9048.
19 B. Kolp, H. Viebrock, A. von Zelewsky and D. Abeln, *Inorg. Chem.*, 2001, **40**, 1196.
20 (*a*) C.-M. Che, W.-T. Tang, W.-T. Wong, H.-W. Lam and T.-F. Lai, *J. Chem. Soc., Dalton Trans.*, 1990, 2077; (*b*) C.-M. Che, T.-F. Lai and K.-Y. Wong, *Inorg. Chem.*, 1987, **26**, 2289.
21 W. Levason, J. J. Quirk and G. Reid, *Acta Crystallogr., Sect. C*, 1997, **53**, 1224.
22 W. A. Nugent and B. L. Haymore, *Coord. Chem. Rev.*, 1980, **31**, 123.

23 (*a*) R. A. Henderson, G. Davies, J. R. Dilworth and R. N. F. Thorneley, *J. Chem. Soc., Dalton Trans.*, 1981, 40; (*b*) M. W. Bishop, J. Chatt, J. R. Dilworth, M. B. Hursthouse and M. Motevalle, *J. Less-Common Met.*, 1977, **54**, 487.
24 (*a*) R. Danton, E. Schweda and J. Strahle, *Z. Naturforsch., B: Anorg. Chem., Org. Chem.*, 1984, **39B**, 733; (*b*) J. Chatt and B. T. Heaton, *J. Chem. Soc. A*, 1971, 705.
25 P. A. Shapley, Z.-Y. Own and J. C. Huffman, *Organometallics*, 1986, **5**, 1269.
26 P. A. Shapley, H. S. Kim and S. R. Wilson, *Organometallics*, 1988, **7**, 928.
27 W. R. Murphy, Jr., K. Takeuchi, M. H. Barley and T. J. Meyer, *Inorg. Chem.*, 1986, **25**, 1041.
28 W.-H. Chiu, C.-X. Guo, K.-K. Cheung and C.-M. Che, *Inorg. Chem.*, 1996, **35**, 540.
29 D. Sellmann, M. W. Wemple, W. Donaubauer and F. W. Heinemann, *Inorg. Chem.*, 1997, **36**, 1397.
30 (*a*) S. Minakata, T. Ando, M. Nishimura, I. Ryu and M. Komatsu, *Angew. Chem., Int. Ed.*, 1998, **37**, 3392; (*b*) J. Du Bois, J. Hong, E. M. Carreira and M. W. Day, *J. Am. Chem. Soc.*, 1996, **118**, 915.
31 P.-H. Ko, PhD Thesis, The University of Hong Kong, 1997.
32 J. C. Lee Jr., A. L. Rheingold, B. Muller, P. S. Pregosin and R. H. Crabtree, *J. Chem. Soc., Chem. Commun.*, 1994, 1021.
33 W.-H. Leung, T. S.-M. Hun, K.-N. Hui, I. D. Williams and D. Vanderveer, *Polyhedron*, 1996, **15**, 421.